

Neutralization of Streptozotocin Induced Diabetic Retinopathy by Punarnavine in Rat

Parmar Bhumika J, Mihir Y Parmar*, Kautuk Shah, Salaj Khare, Zalak Dave, Imtiyaz Baghban, Kaish Pathan, Palak Landge, Devanshi Sharma and Paswan Praveen Kumar

Department of Pharmacology, Krishna School of Pharmacy and Research (Formerly, Babaria Institute of Pharmacy), Drs. Kiran and Pallavi Patel Global University, Krishna Edu Campus, Varnama, Vadodara, Gujarat, India

***Corresponding Author:** Mihir Y Parmar, HOD and Professor, Department of Pharmacology, Krishna School of Pharmacy and Research (Formerly, Babaria Institute of Pharmacy), Drs. Kiran and Pallavi Patel Global University, Krishna Edu Campus, Varnama, Vadodara, Gujarat, India.

Received: December 05, 2024; **Published:** January 22, 2025

Abstract

Diabetic retinopathy (DR) is a severe complication of diabetes mellitus characterized by oxidative stress and impaired retinal vascular function. This study investigates the therapeutic potential of Punarnavine, an experimental drug, in mitigating DR in streptozotocin (STZ)-induced diabetic rats. Animals were treated with low (DR+PNLD) and high (DR+PNHD) doses of Punarnavine, and various biochemical assays were conducted to evaluate oxidative stress markers and antioxidant enzyme activities. Treatment with Punarnavine significantly reduced malondialdehyde (MDA) levels, indicative of decreased lipid peroxidation, in both DR+PNLD (2.48 nmol/mg protein, SD = 0.56) and DR+PNHD (2.22 nmol/mg protein, SD = 0.18) groups compared to untreated DR rats. Catalase activity was enhanced in DR+PNHD rats (71.42 units/mg protein, SD = 0.63), showing robust antioxidant defence mechanisms. Similarly, superoxide dismutase (SOD) activity was significantly elevated in DR+PNHD rats (26.1 units/mg protein, SD = 1.28), underscoring effective antioxidant capacity. Glutathione (GSH) activity was also markedly increased in DR+PNHD rats (46.55 units/mg protein, SD = 1.17), further supporting enhanced antioxidant defences. Assessment of vascular permeability as a measure of retinal dysfunction revealed variable responses: DR+PNLD (20.48 µg/mL, SD = 1.05) displayed mixed outcomes, whereas DR+PNHD (20.43 µg/mL, SD = 0.59) showed moderate improvement compared to untreated DR rats. In conclusion, Punarnavine exhibits potent antioxidant properties by reducing oxidative stress markers and enhancing antioxidant enzyme activities in STZ-induced diabetic retinopathy. While high-dose Punarnavine shows promising efficacy in improving retinal antioxidant defences and reducing vascular dysfunction, further studies are warranted to optimize therapeutic outcomes for diabetic retinopathy management.

Keywords: Diabetic Retinopathy; Punarnavine; Oxidative Stress; Antioxidant Enzymes; Streptozotocin

Introduction

Introduction to diabetic retinopathy

Diabetic retinopathy is an eye condition linked to diabetes that affects the retina, the light-sensitive tissue at the back of the eye. Prolonged high blood sugar levels can harm the small blood vessels in the retina, leading to vision issues. Early stages may be asymptomatic, but as it progresses, symptoms like blurred vision, floaters, and potentially blindness can develop if untreated. Regular eye exams for people with diabetes are crucial for early detection and management of diabetic retinopathy. Diabetic retinopathy is a microvascular disease resulting

from long-term effects of diabetes mellitus. It's a leading cause of severe vision loss in working-age adults in the Western world. Timely intervention is key to preventing blindness from diabetic retinopathy. By 2050, an estimated 16 million Americans may have diabetic retinopathy, with around 3.4 million at risk of vision-threatening complications. Effective glycaemic control has been validated in trials like the UK Prospective Diabetes Study and Diabetes Control and Complication Trial. Poorly managed diabetes can lead to various eye problems such as cataracts, glaucoma, and diabetic retinopathy, which remains the most common and serious ocular complication. Factors contributing to worsening diabetic retinopathy include poor glycaemic control, uncontrolled hypertension, dyslipidaemia, nephropathy, male gender, and obesity. Characteristic signs of diabetic retinopathy include microaneurysms, exudates, diabetic macular edema (DME), and new vessels in proliferative diabetic retinopathy (PDR). Regular monitoring and early treatment are crucial in preventing vision loss from this condition [1,2].

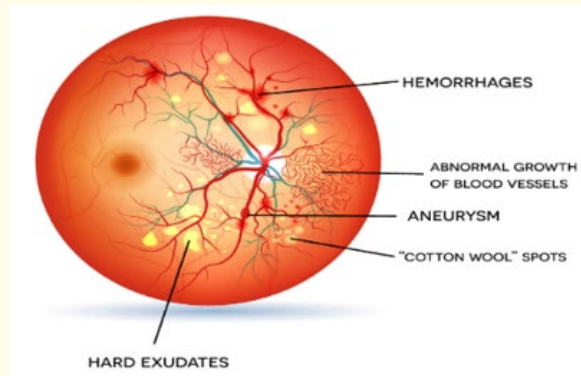


Figure 1: Pathogenesis of diabetic retinopathy.

Introduction to punarnava

Boerhavia diffusa (BD) Linn., a member of the Nyctaginaceae family, is esteemed in traditional Indian medicine and various regions worldwide, including Southern America and Africa. Its roots are particularly valued for their use in treating gastrointestinal, hepatoprotective, and gynaecological conditions across these regions, as well as in Ayurvedic medicine where it features prominently in over 35 formulations. Ayurveda categorizes BD as a "rasayana" herb, highlighting its purported properties such as anti-aging effects, rejuvenation, vitality enhancement, intelligence support, and disease prevention. These attributes suggest BD enhances the body's resilience against illnesses, providing hepatoprotection and immunomodulation. BD has been extensively researched for its chemical composition and therapeutic potential. Its roots yield a diverse array of bioactive compounds including rotenoids (a unique class of isoflavonoids), flavonoids, flavonoid glycosides, xanthenes, purine nucleoside, lignans, ecysteroids, and steroids. Animal studies and clinical trials have demonstrated BD's pharmacological activities, such as immunomodulation, hepatoprotection, antifibrinolytic effects, anticancer properties, antidiabetic effects, anti-inflammatory actions, and diuretic effects, BD is a well-established medicinal plant with a rich history of use in traditional medicine systems globally. Its roots contain a plethora of bioactive compounds that contribute to its therapeutic efficacy. Ongoing research continues to explore and validate its medicinal applications, reinforcing its status as a valuable herb in both traditional and modern medicinal practices [3-6].



Figure 2: Plant Boerhavia diffusa.

Class	Compounds
Alkaloid	Punarnavine
Rotenoids	Boeravinone A-F
Glycoside	Hypoxanthine 9-L-arabinofuranoside, Hentriacontane, β -sitosterol and ursolic acid, Punarnavoside, 111 C-methylflavone 5,7-dihydroxy-3',4'-dimethoxy- 6,8- dimethylflavone, β -ecdysone, triacontane, β -sitosterol- β -D-glucoside
Acids	Tetracosanoic, Hexacosanoic, Stearic, Palmitic, Arachidic Acids
Lignans	Liriodendrin Syringaresinol mono- β - D-glucoside Glycoprotein
Lipids	5-methyleicos-4-ene Eicos-4-ene 4-methyloctadec-3-ene 4-methylnonadecylbenzene
Phenolic compounds	3,4-dihydroxy-5-methoxycinnamoylrhamnoside, Quercetin 3-O-rhamnosyl (1→6) galactoside (quercetin 3-O-robinobioside), Quercetin 3-O-(2''- rhamnosyl)-robinobioside, Kaempferol 3-O-(2''-rhamnosyl)-robinobioside, 3,5,4'- rihydroxy-6,7-dimethoxyflavone 3-Ogalactosyl(1→2)glucoside [eupalitin 3-Ogalactosyl(1→2) glucoside], Caffeoyltartaric acid, Kaempferol 3-O-robinobioside, Eupalitin 3-O-galactoside, Quercetin, Kaempferol, 6, 9, 11-Trihydroxy-6a 12a-dehydrorotenoid (coccineone B)

Table 1: Chemical constituents isolated from Boerhavia diffusa [7].

Introduction to punarnavine

Punarnavine (PN) is a quinolizidine alkaloid found in *B. diffusa*. It is isolated from the whole plant-in the alkaloidal fraction. Syringaresinol mono- β -D-glucoside along with PN was also isolated from roots of BD [16]. The chemical formula of PN is $C_{18}H_{15}NO_4$ and its molecular weight is 309.32 Da [7-9].

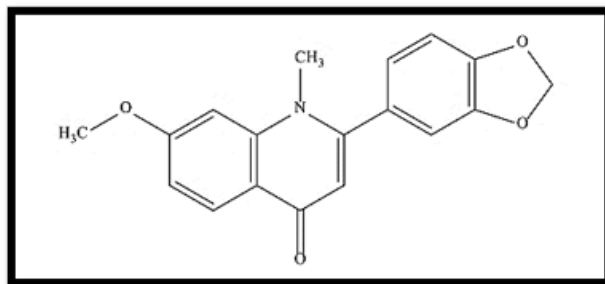


Figure 3: Chemical structure of punarnavine.

Purpose of the Study

The purpose of this study is to summarize the preclinical diabetic retinopathy potential of PN as a newly emerged drug candidate from natural source. The source of this plant is already used in traditional medicine. Therefore, this natural product will be a new approach of anticancer drug discovery.

Material and Methods

Animals

The purpose of this study was to investigate the effects of punarnavine in neutralizing streptozotocin (STZ)-induced diabetic retinopathy in rats. Specifically, 8-10 weeks old Wistar rats were sourced from an approved CPCSEA registered organization, Sun Pharma Pvt Ltd. Upon arrival, the rats were housed in standard laboratory cages with corncob bedding, under controlled environmental conditions: a temperature of $22 \pm 1^\circ\text{C}$, relative humidity of $50 \pm 5\%$, and a 12-hour light/dark cycle. Four rats were housed per cage, receiving standard laboratory chow (Purina 5001) and water ad libitum. The study adhered strictly to the guidelines of the Institutional Animal Care and Use Committee (IACUC) at Krishna School of Pharmacy and Research, KPGU, and was approved under protocol number KSP/IEAC/2024/01. Ethical considerations were paramount, following the guidelines set forth by the Committee for the Purpose of Control and Supervision of Experiments on Animals (CPCSEA). This ensured ethical treatment, proper housing, and care of the animals throughout the study. Measures were taken to minimize pain and distress through the use of appropriate anaesthesia and humane endpoints, reflecting a commitment to responsible animal research practices.

Experimental groups

The animals will be randomly divided into five groups, each containing six rats ($n = 6$): Normal Control Group (NC), which will be non-diabetic and receive no treatment; Diabetic Control Group (DC), which will be diabetic and receive no treatment; Low Dose Punarnavine Treatment Group (DC+PNLD), which will be diabetic and treated with a low dose of Punarnavine; High Dose Punarnavine Treatment Group (DC+PNHD), which will be diabetic and treated with a high dose of Punarnavine; and Standard Drug Treatment Group (DC+SM), which will be diabetic and treated with metformin.

Preliminary work

IR identification

FTIR spectra of punarnavine obtain using Agilent Technologies FTIR Cary 630 with ATR sampling using EZ-PROBE software. The range is from 4000 - 650.

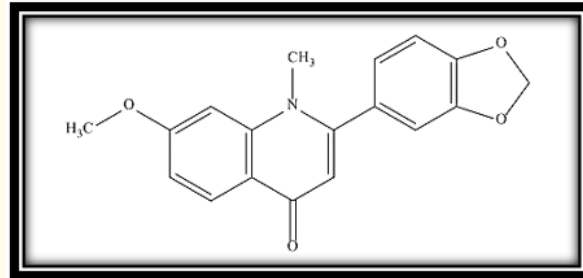


Figure 4: Chemical structure of punarnavine.

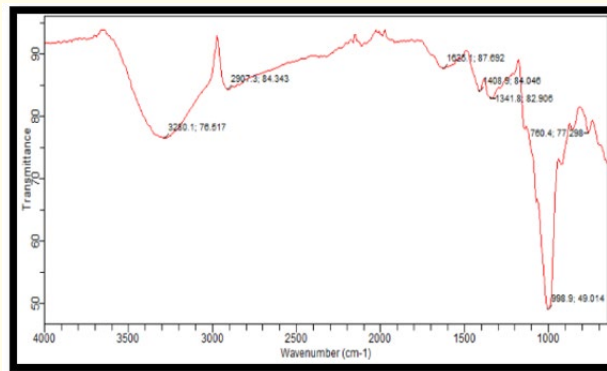


Figure 5: FTIR spectra of punarnavine.

Interpretation of FTIR spectrum of punarnavine

The FTIR spectrum of Punarnavine (Figure 11) shows several characteristic absorption bands that confirm the presence of specific functional groups in the molecule. The broad absorption band observed around 3360 cm⁻¹ is indicative of the O-H stretching vibration, suggesting the presence of hydroxyl groups. The peaks observed in the region of 2900-3000 cm⁻¹ correspond to the C-H stretching vibrations of the methyl and methylene groups.; A strong absorption band at approximately 1700 cm⁻¹ is attributed to the C=O stretching vibration, confirming the presence of a carbonyl group. The absorption bands around 1600 cm⁻¹ can be associated with the C=C stretching vibrations of aromatic rings present in the structure of Punarnavine. Additional peaks observed between 1050-1300 cm⁻¹ correspond to the C-O stretching vibrations; The FTIR data corroborates the chemical structure of punarnavine, as shown in figure 10. This spectrum provides vital information about the functional groups present in the compound, aiding in the comprehensive understanding of its chemical composition.

Sr No.	Functional Group	Wave Number [cm ⁻¹]
	O-H Stretching (hydroxyl groups)	3360
	C-H Stretching (methyl and methylene group)	2900-3000
	C=O Stretching (carbonyl group)	1700
	C=C Stretching	1600
	C-O Stretching	1050-1300

Table 2: Summary of Interpretation of IR spectra of punarnavine.

Solubility study of punarnavine in various solvents

Introduction to solubility study

Objective: State the purpose of studying the solubility of punarnavine in different solvents. For example, “The solubility of punarnavine was evaluated in various solvents to determine its optimal medium for further pharmaceutical applications”.

Methodology

Materials and Methods: Describe the solvents used (distilled water, normal saline, DMSO, etc.) and the procedure for measuring solubility. For example, “Punarnavine solubility was measured in distilled water, normal saline, and DMSO by dissolving a known quantity in a fixed volume of each solvent and assessing the saturation point”.

Results



Figure 6: Solubility of punarnavine in distilled water.

Solvent	Solubility (mg/mL)
Double Distilled Water	0.8 mg/ml
Normal Saline	2.0 mg/ml
DMSO	15.0 mg/ml

Table 3: Presentation of the solubility data of punarnavine in double distilled water, normal saline, DMSO.

Analysis: Punarnavine exhibited the highest solubility in DMSO (15.0 mg/mL), followed by normal saline (2.0 mg/mL), and the lowest in double-distilled water (0.8 mg/mL).

Justification of using distilled water as a solvent

Using distilled water as a solvent for oral dosing in rats is often preferred due to its safety, simplicity, and lack of confounding variables. It avoids the potential complications associated with DMSO toxicity and the introduction of electrolytes from normal saline, making it a suitable choice for many experimental setups. However, this decision should always be validated with specific experimental requirements, considering the solubility of the compound and the goals of the study.

Evaluation parameters

Physical parameters	Biochemical parameters	Histopathology
Body weight	Fasting Blood glucose levels	Retina
Food Consumption	Haemoglobin A1c (HbA1c)	Pancreas
Fluid Consumption (water)	Serum Insulin	Liver
Urine excretion	Lipid profile	-
-	Antioxidant parameters	-
-	Inflammatory markers	-
-	Retinal Vascular Permeability	-

Table 4: List of biochemical parameters to evaluate in study protocol.

Thiobarbituric acid reactive substances (TBARS) assay for estimating malondialdehyde (MDA)

To assess malondialdehyde (MDA) production as a marker of oxidative stress, a precise method is followed. First, prepare two reagents: a 0.67% thiobarbituric acid solution in Tris-HCl buffer (pH 7) and a 10% trichloroacetic acid solution. Create a blank solution by mixing 2 mL of trichloroacetic acid with 1 mL of distilled water, centrifuge to remove any precipitates, and then add 2 mL of thiobarbituric acid solution to the supernatant. For the test solution, mix 2 mL of trichloroacetic acid with 1 mL of sample homogenate, centrifuge, and combine the supernatant with 2 mL of thiobarbituric acid solution. Heat both solutions (95°C for 10 minutes or 80°C for 40 minutes) and cool rapidly on ice to stop the reaction. Measure absorbance of the test solution at 535 nm against the blank using a spectrophotometer. Higher absorbance values indicate increased MDA levels, reflecting greater oxidative stress. This method quantitatively evaluates oxidative damage, crucial for studying oxidative stress mechanisms and assessing antioxidant treatments in biological systems [19].

Estimation of catalase activity: Spectrophotometric analysis using hydrogen peroxide decomposition

To assess catalase activity, prepare a supernatant or extract containing the enzyme from tissue homogenates or biological samples. Combine 0.1 ml of this enzyme sample with 1.9 ml of 50 mM phosphate buffer (pH 7.0) in a cuvette or test tube, as this buffer optimally supports catalase activity. Add 1.0 ml of freshly prepared 30 mM hydrogen peroxide (H₂O₂) to initiate the reaction, ensuring the enzyme is not saturated for measurable enzymatic activity. Immediately start measuring the absorbance of the reaction mixture at 240 nm using a spectrophotometer; this wavelength corresponds to hydrogen peroxide breakdown catalyzed by catalase. Record the decrease in absorbance over 3 minutes; the rate of absorbance decrease reflects catalase activity. Calculate catalase activity quantitatively based on the rate of absorbance decrease at 240 nm, typically reported as micromoles of hydrogen peroxide decomposed per minute per milligram of protein (μmol/min/mg protein). This assay offers a reliable method to evaluate catalase function, providing insights into antioxidant defences and oxidative stress responses in biological samples [21,22].

Estimation of superoxide dismutase (SOD) activity: Spectrophotometric analysis using superoxide radical scavenging

To conduct a spectrophotometric assay for Superoxide Dismutase (SOD) enzyme activity, prepare a tissue homogenate and obtain a supernatant by centrifugation. Create a blank using distilled water in a clean cuvette and measure absorbance at 540 nm to establish background levels. Prepare standard SOD solutions with known activities (5 to 160 units/ml) to construct a standard curve. Mix each sample with carbonate buffer (pH 10.2) and EDTA to stabilize pH and inhibit metal-catalyzed reactions. Introduce a superoxide anion generator, such as epinephrine, to initiate the reaction and immediately measure initial absorbance at 480 nm. After adding the enzyme sample, incubate for a specified time (5-20 minutes) and measure final absorbance at 480 nm. Calculate SOD activity using absorbance values, adjusting for dilution factors and referencing the standard curve for unknown samples. This method ensures precise measurement of SOD activity via spectrophotometry, offering insights into the antioxidant potential of tested tissue homogenates [23,24].

Estimation of glutathione (GSH) levels: Spectrophotometric analysis using glutathione reductase and DTNB method

The method for assessing glutathione (GSH) levels in Wistar rat retinal tissues begins with homogenization and centrifugation to obtain a supernatant containing soluble proteins, including GSH. Simultaneously, blank solutions are prepared with distilled water in cuvettes or microplate wells, and their absorbance at approximately 412 nm is measured to establish baseline readings. GSH standards of known concentrations (typically 0 to 100 μM) are prepared using buffered solutions to stabilize pH and enzyme activity, forming a reference curve for quantification. Samples and standards are mixed with carbonate buffer (pH 7.4) and DTNB to initiate the reaction, and initial absorbance is measured. Glutathione reductase and NADPH are added to convert oxidized glutathione (GSSG) to reduced glutathione (GSH), with incubation at a controlled temperature (e.g. 25°C) while monitoring absorbance over 3 minutes. Final absorbance values are recorded and used to calculate ΔA for each sample and standard. GSH concentrations in samples are determined by referencing the standard curve, accounting for dilution factors and sample volumes. Quality control ensures measurements fall within the linear range of the standard curve and includes duplicate or triplicate measurements for reproducibility. Statistical analysis compares GSH concentrations across experimental groups (e.g., diabetic retinopathy vs. controls), providing insights into tissue antioxidant capacity and treatment efficacy in oxidative stress conditions [25].

Procedure for retinal vascular permeability studies

In studies assessing retinal vascular permeability using the Evans blue dye technique, the procedure is critical for evaluating blood-retinal barrier (BRB) integrity. Experimental rats are deeply anesthetized, and Evans blue dye (30 mg/mL in saline) is administered intravenously via the tail vein at a dosage of 45 mg/kg over 10 seconds. Blood samples are collected from the left ventricle before perfusion to determine the time-averaged plasma concentration of Evans blue dye. Plasma samples are processed by centrifugation to separate plasma from cellular components and diluted 1/10,000 in formamide. Spectrophotometric measurements at 620 nm and 740 nm quantify dye absorbance, reflecting its concentration in plasma. After circulating for 2 hours, rats are euthanized, and their eyes are perfused with 1% paraformaldehyde in citrate buffer to fix retinal tissues under constant pressure. Retinas are carefully dissected and incubated in formamide at 70°C for 18 hours to extract Evans blue dye. Extracted samples undergo ultracentrifugation, and supernatants are analyzed spectrophotometrically at 620 nm and 740 nm to measure dye concentration. This method provides a systematic approach to evaluating BRB integrity and understanding the dynamics of retinal vascular permeability in disease models like diabetic retinopathy [27,28].

Histopathological examination of retina, pancreas and liver

The histopathological evaluation of the retina and retinal tissue was conducted through a series of meticulous steps. Rats were humanely euthanized, and their eyes were carefully enucleated and immediately placed in 10% neutral-buffered formalin for 24-48 hours to preserve retinal structure. The eyes were then washed in phosphate-buffered saline (PBS) to remove excess fixative, dehydrated through a graded series of ethanol, cleared in xylene, and infiltrated with melted paraffin wax. The eyes were embedded in paraffin to

create solid blocks, which were then trimmed and sectioned using a microtome to obtain thin slices of about 4-5 micrometres. These retinal sections were floated on a warm water bath to flatten them and mounted on glass slides. The sections were deparaffinized in xylene, rehydrated through ethanol, and stained with Haematoxylin and Eosin (H&E) to visualize retinal structure. Additional staining, such as Periodic Acid-Schiff (PAS) or immunohistochemical stains, was performed as needed. After staining, the sections were dehydrated again in ethanol, cleared in xylene, and mounted with coverslips using a suitable mounting medium. The prepared slides were examined under a light microscope, and detailed evaluations of the retinal layers, including the ganglion cell layer, inner and outer nuclear layers, and the photoreceptor layer, were conducted. Photomicrographs of the sections were captured, and a comprehensive histopathological report documenting the findings and any observed pathological changes was prepared.

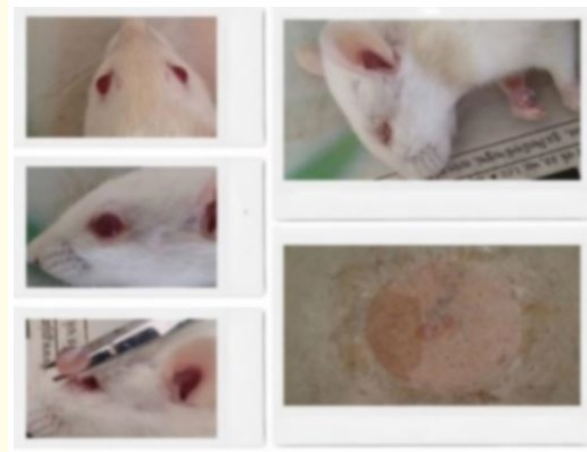


Figure 7: Dissection reveals pathological features of diabetic retinopathy in rat model.

Result and Discussion

Summary of physical parameters measurement

Physical parameter	Treatment group's Mean and SD				
	NC	DC	DC+SM	DC+PNLD	DC+PNHD
Blood Glucose	109.72 ± 6.67 mg/dL	207.05 ± 28.58 mg/dL	186.47 ± 52.79 mg/dL	253.63 ± 120.22 mg/dL	281.12 ± 138.24 mg/dL
Body Weight	265.5 ± 5.579601 gm	205.5 ± 22.39482 gm	220.6 ± 28.75937 gm	223.5 ± 24.83767 gm	220.4 ± 24.78893 gm
Food Consumption	49.05 ± 2.36 gm	26.69 ± 5.24 gm	31.55 ± 7.99 gm	35.76 ± 8.89 gm	33.94 ± 9.26 gm
Fluid Consumption	27.86 ± 1.88 ml	51.88 ± 16.87 ml	55.38 ± 16.81 ml	47.33 ± 13.44 ml	51.59 ± 13.43 ml
Urinary Excretion	15.66 ± 1.10 ml	22.94 ± 4.81 ml	19.02 ± 5.72 ml	17.38 ± 5.43 ml	19.46 ± 5.79 ml

Table 5: Summary of physical parameters measurement.

Summary of lipid profile measurement

Lipid profile	Treatment group's mean and SD				
	NC	DC	DC+SM	DC+PNLD	DC+PNHD
%Hba1c	7.4 ± 0.2646%	8.2167 ± 0.1972%	7.125 ± 0.5998%	6.75 ± 0.4682%	7 ± 0.0707%
Serum Insulin	12.3333 ± 0.7652 units/mL	9.8233 ± 0.5752 units/mL	11.925 ± 0.5801 units/mL	11.2167 ± 0.2478 units/mL	11.6125 ± 0.3646 units/mL
Cholesterol	229.13 ± 23.6823 mg/dL	441.28 ± 118.9308 mg/dL	240.5 ± 33.3683 mg/dL	303.25 ± 31.7578 mg/dL	183.23 ± 59.9214 mg/dL
Total Protein	1.83 ± 0.4119 g/dL	3.12 ± 0.1646 g/dL	1.77 ± 0.2793 g/dL	1.59 ± 0.3610 g/dL	1.71 ± 0.1816 g/dL
Uric Acid	5.97 ± 0.2132 mg/dL	8.63 ± 0.9762 mg/dL	5.94 ± 0.3042 mg/dL	6.52 ± 0.5740 mg/dL	5.52 ± 0.2690 mg/dL
Serum Triglyceride	204.39 ± 7.836 mg/dL	390.08 ± 48.592 mg/dL	213.73 ± 20.548 mg/dL	285.22 ± 25.970 mg/dL	212.88 ± 9.129 mg/dL
Serum Albumin	3.64 ± 0.0601 g/dL	4.91 ± 0.2834 g/dL	3.74 ± 0.1361 g/dL	3.89 ± 0.6717 g/dL	3.32 ± 0.1489 g/dL

Table 6: Summary of lipid profile measurement.

Results of antioxidant capacity

Comparison of malondialdehyde (MDA) activity levels in different treatment groups

Group	Mean MDA Activity (nmol/mg protein)	Standard Deviation (nmol/mg protein)
NC	1.03	± 0.26
DC	3.6	± 0.76
DC+SM	1.92	± 0.52
DC+PNLD	2.48	± 0.56
DC+PNHD	2.22	± 0.18

Table 7: Comparison of malondialdehyde (MDA) activity levels in different treatment groups.

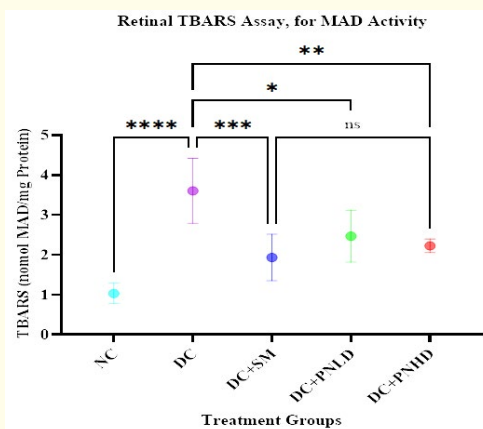


Figure 8: The bar graph illustrates the measurement of retinal Malondialdehyde (MDA) activity (nmol/mg protein) in diabetic retinopathy (DR) rats treated with punarnavine at low dose (DR+PNLD) and high dose (DR+PNHD), compared to untreated DR rats (Control). Error bars represent standard deviation (SD). *p < 0.05 vs. DR (Control).

The study evaluated malondialdehyde (MDA) activity via the Retinal TBARS assay (nmol/mg protein) in Wistar rats to assess oxidative stress in diabetic retinopathy (DR). Normal controls (NC) had MDA levels of 1.03 nmol/mg protein (SD = 0.26), contrasting sharply with DR rats (3.6 nmol/mg protein, SD = 0.76), indicating heightened oxidative stress. Treatment with standard metformin (DR+SM) reduced MDA to 1.92 nmol/mg protein (SD = 0.52), while low (DR+PNLD) and high dose (DR+PNHD) experimental drugs achieved 2.48 nmol/mg protein (SD = 0.56) and 2.22 nmol/mg protein (SD = 0.18), respectively. These findings highlight therapeutic potential in managing oxidative stress and preserving retinal health in diabetic conditions, meriting further clinical exploration of antioxidant therapies.

Comparison of catalase activity levels in different treatment groups

Group	Mean Catalase Activity (units/mg protein)	Standard Deviation (units/mg protein)
NC	80.08	± 6.31
DR	43.73	± 3.83
DR+SM	60.37	± 6.18
DR+PNLD	55.88	± 1.79
DR+PNHD	71.42	± 0.63

Table 8: Comparison of catalase activity levels in different treatment groups.

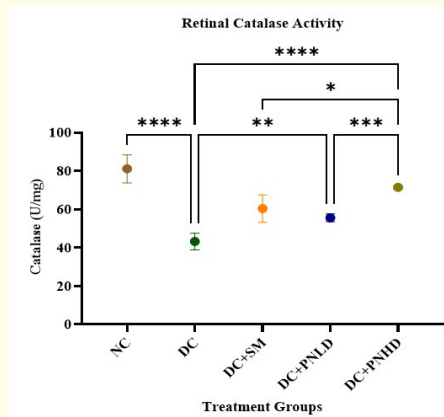


Figure 9: The graph illustrates the measurement of retinal catalase activity (units/mg protein) in diabetic retinopathy (DR) rats treated with punarnavine at low dose (DR+PNLD) and high dose (DR+PNHD), compared to untreated DR rats (Control).

Error bars represent standard deviation (SD). *p < 0.05 vs. DR (Control).

The study assessed catalase activity in Wistar rats under various conditions, focusing on diabetic retinopathy (DR) and therapeutic interventions. Normal controls (NC) had robust catalase activity (mean = 80.08 units/mg protein, SD = 6.31), contrasting sharply with DR rats showing reduced activity (mean = 43.73 units/mg protein, SD = 3.83), indicating oxidative stress in diabetes. Rats treated with standard medication (DR+SM) showed moderate improvement (mean = 60.37 units/mg protein, SD = 6.18), while low-dose experimental drug treatment (DR+PNLD) resulted in effective enhancement (mean = 55.88 units/mg protein, SD = 1.79). High-dose experimental drug treatment (DR+PNHD) exhibited the highest activity (mean = 71.42 units/mg protein, SD = 0.63), highlighting significant antioxidant enhancement. These results underscore the impact of diabetic retinopathy on catalase activity and suggest potential therapeutic strategies to bolster antioxidant defences in managing diabetic complications, particularly retinopathy.

Comparison of superoxide dismutase (SOD) level in different treatment groups

Group	Mean SOD Activity (units/mg protein)	Standard Deviation (units/mg protein)
NC	24.29	± 2.35
DR	14.14	± 2.32
DR+SM	20.71	± 2.34
DR+PNLD	22.86	± 2.12
DR+PNHD	26.1	± 1.28

Table 9: Comparison of superoxide dismutase (SOD) level in different treatment groups.

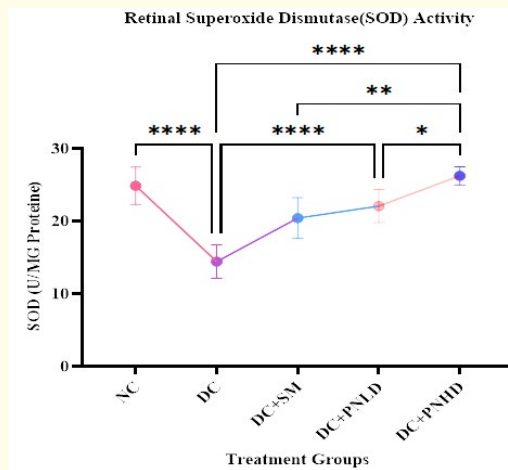


Figure 10: The bar graph illustrates the measurement of retinal superoxide dismutase (SOD) activity (units/mg protein) in diabetic retinopathy (DR) rats treated with punarnavine at low dose (DR+PNLD) and high dose (DR+PNHD), compared to untreated DR rats (Control). Error bars represent standard deviation (SD). *p < 0.05 vs. DR (Control).

The study investigated superoxide dismutase (SOD) activity in Wistar rats across different experimental groups to assess its modulation in diabetic retinopathy (DR) and potential therapeutic interventions. Normal controls (NC) showed stable SOD activity (mean = 24.29 units/mg protein, SD = 2.35), indicative of healthy antioxidant function. Rats with diabetic retinopathy (DR) exhibited significantly lower SOD activity (mean = 14.14 units/mg protein, SD = 2.32), underscoring oxidative stress in the disease. Treatment with standard metformin (DR+SM) partially restored SOD activity (mean = 20.71 units/mg protein, SD = 2.34), while low-dose experimental drug treatment (DR+PNLD) further improved SOD levels (mean = 22.86 units/mg protein, SD = 2.12). High-dose experimental drug treatment (DR+PNHD) showed the highest SOD activity (mean = 26.1 units/mg protein, SD = 1.28) among all groups, indicating substantial enhancement of antioxidant defences. These findings highlight diabetic retinopathy’s impact on antioxidant defences, emphasizing potential therapeutic strategies to enhance SOD activity in managing oxidative stress associated with the condition.

Comparison of glutathione (GSH) level in different treatment groups

Group	Mean GSH Activity (units/mg protein)	Standard Deviation (units/mg protein)
NC	48.73	± 5.49
DR	26.85	± 4.32
DR+SM	36.67	± 3.30
DR+PNLD	38.88	± 3.10
DR+PNHD	46.55	± 1.17

Table 10: Comparison of glutathione (GSH) level in different treatment groups.

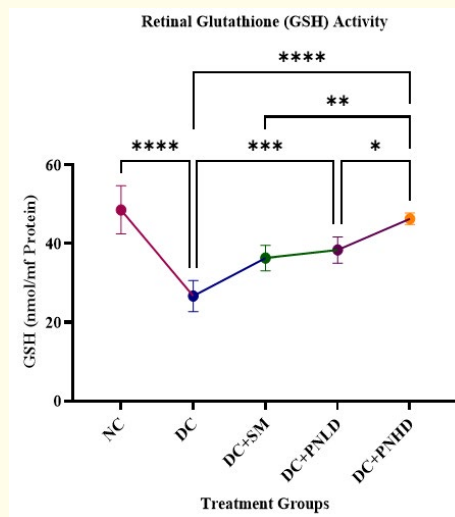


Figure 11: The graph illustrates the measurement of retinal glutathione (GSH) activity (units/mg protein) in diabetic retinopathy (DR) rats treated with punarnavine at low dose (DR+PNLD) and high dose (DR+PNHD), compared to untreated DR rats (Control). Error bars Represent standard deviation (SD). * $p < 0.05$ vs. DR (Control).

The study investigated glutathione (GSH) activity in Wistar rats across experimental groups to assess its modulation in diabetic retinopathy (DR) and potential treatments. Normal controls (NC) exhibited robust GSH activity (mean = 48.73 units/mg protein, SD = 5.49), indicating healthy antioxidant defence. Rats with diabetic retinopathy (DR) showed reduced GSH activity (mean = 26.85 units/mg protein, SD = 4.32), highlighting oxidative stress in diabetes. Treatment with standard medication (DR+SM) partially restored GSH activity (mean = 36.67 units/mg protein, SD = 3.30), while low-dose experimental drug treatment (DR+PNLD) further enhanced GSH levels (mean = 38.88 units/mg protein, SD = 3.10), indicating promising therapeutic potential. High-dose experimental drug treatment (DR+PNHD) resulted in the highest GSH activity (mean = 46.55 units/mg protein, SD = 1.17), demonstrating robust enhancement of antioxidant defences. These findings underscore diabetic retinopathy's impact on GSH activity and highlight the effectiveness of treatments in restoring antioxidant defences, suggesting new avenues for managing oxidative stress and diabetic complications like retinopathy.

Comparison of retinal vascular permeability in different treatment groups

Group	Mean Vascular Permeability ($\mu\text{g/mL}$)	Standard Deviation ($\mu\text{g/mL}$)
NC	1.03 $\mu\text{g/mL}$	$\pm 0.26 \mu\text{g/mL}$
DR	24.67 $\mu\text{g/mL}$	$\pm 0.66 \mu\text{g/mL}$
DR+SM	18.53 $\mu\text{g/mL}$	$\pm 0.38 \mu\text{g/mL}$
DR+PNLD	20.48 $\mu\text{g/mL}$	$\pm 1.05 \mu\text{g/mL}$
DR+PNHD	20.43 $\mu\text{g/mL}$	$\pm 0.59 \mu\text{g/mL}$

Table 11: Comparison of retinal vascular permeability in different treatment groups.

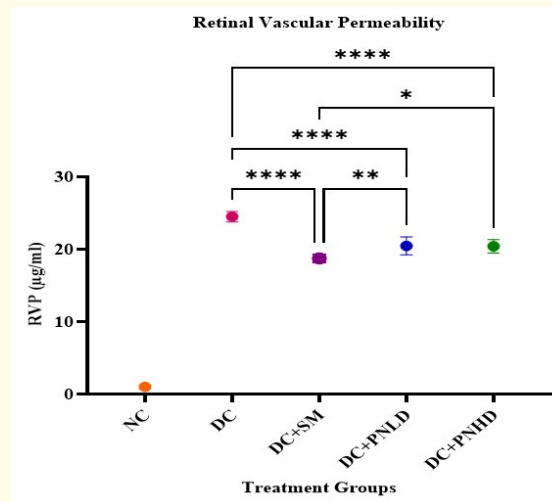


Figure 12: The graph illustrates the measurement of vascular permeability ($\mu\text{g/mL}$) in diabetic retinopathy rats treated with low dose punarnavine (DR+PNLD) and high dose punarnavine (DR+PNHD), compared to untreated DR rats. Error bars represent standard deviation (SD). * $p < 0.05$ vs. DR (Control).

The study investigated retinal vascular permeability in Wistar rats across experimental groups to assess changes associated with diabetic retinopathy (DR) and potential therapies. Normal controls (NC) had a mean vascular permeability of 1.03 $\mu\text{g/mL}$ (SD = 0.26), indicating healthy retinal blood vessel integrity. Rats with diabetic retinopathy (DR) exhibited significantly increased vascular permeability, averaging 24.67 $\mu\text{g/mL}$ (SD = 0.66), reflecting compromised blood-retinal barrier function. Treatment with standard medication (DR+SM) reduced vascular permeability to 18.53 $\mu\text{g/mL}$ (SD = 0.38), suggesting therapeutic efficacy in mitigating leakage. Low-dose experimental drug treatment (DR+PNLD) showed variable outcomes with a mean of 20.48 $\mu\text{g/mL}$ (SD = 1.05), while high-dose treatment (DR+PNHD) resulted in a mean of 20.43 $\mu\text{g/mL}$ (SD = 0.59), indicating moderate improvement compared to untreated DR rats. These findings underscore diabetic retinopathy's impact on retinal vascular permeability and highlight varied effectiveness of treatments in reducing leakage, emphasizing the need for targeted therapeutic strategies to preserve retinal health and vision in diabetic patients.

Inflammatory bio-markers

C-reactive protein (CRP)

C-reactive protein (CRP) is a sensitive marker of inflammation and systemic response to tissue injury, infection, or chronic diseases. In the context of diabetic retinopathy, inflammation plays a significant role in the progression and severity of retinal damage. Punarnavine, a bioactive compound with therapeutic potential, has shown promising effects in attenuating diabetic complications.

Group	Mean CRP (mg/L)	Standard Deviation (µg/mL)
NC	1.83 µg/mL	± 0.41 µg/mL
DC	3.12 µg/mL	± 0.16 µg/mL
DC+SM	1.77 µg/mL	± 0.28 µg/mL
DC+PNLD	1.59 µg/mL	± 0.36 µg/mL
DC+PNHD	1.71 µg/mL	± 0.18 µg/mL

Table 12: Comparison of retinal CRP activity in different treatment groups.

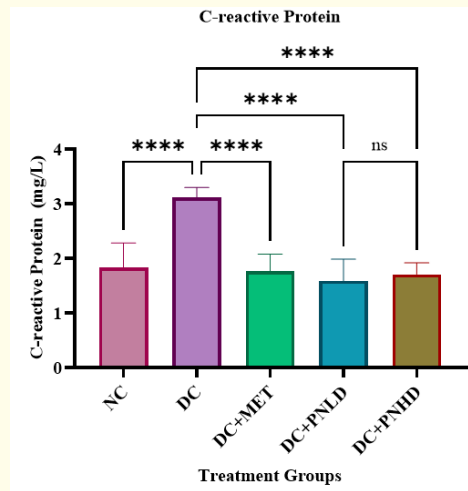


Figure 13: The graph illustrates the measurement of Retinal CRP Activity (mg/dL) in diabetic retinopathy rats treated with low dose punarnavine (DR+PNLD) and high dose punarnavine (DR+PNHD), compared to untreated DR rats. Error bars represent standard deviation **p* < 0.05 vs. DR (Control).

The mean C-reactive protein (CRP) levels varied significantly across the experimental groups following different treatments. The Normal Control group (NC), administered distilled water orally (0.5% w/v), exhibited a mean CRP level of 1.83 ± 0.412 mg/L, ranging from 1.3 mg/L to 2.45 mg/L. In contrast, the Diabetic Control group (DC), induced with STZ (55 mg/kg, intraperitoneal injection), showed a notably higher mean CRP level of 3.12 ± 0.165 mg/L, with a narrower range from 2.9 mg/L to 3.33 mg/L. The STZ + Metformin group (SM), receiving STZ (55 mg/kg) and Metformin (70 mg/kg orally), displayed a mean CRP level of 1.77 ± 0.279 mg/L, with a range from 1.4 mg/L to 2.1 mg/L. Similarly, the STZ + Low Dose Punarnavine group (SLP), treated with STZ and low dose Punarnavine (20 mg/kg orally), had a mean CRP level of 1.59 ± 0.361 mg/L, ranging from 1 mg/L to 1.95 mg/L. Conversely, the STZ + High Dose Punarnavine group (SHP), treated with STZ and high dose Punarnavine (40 mg/kg orally), showed a mean CRP level of 1.71 ± 0.182 mg/L, with a range from 1.5 mg/L to 2 mg/L. These results underscore the varying impact of treatments on CRP levels, highlighting both the central tendency and variability within each group. This paragraph succinctly summarizes how different treatments affect CRP levels, emphasizing the mean values and the range of variability observed across the experimental groups.

Histological examination and pathological features of retina

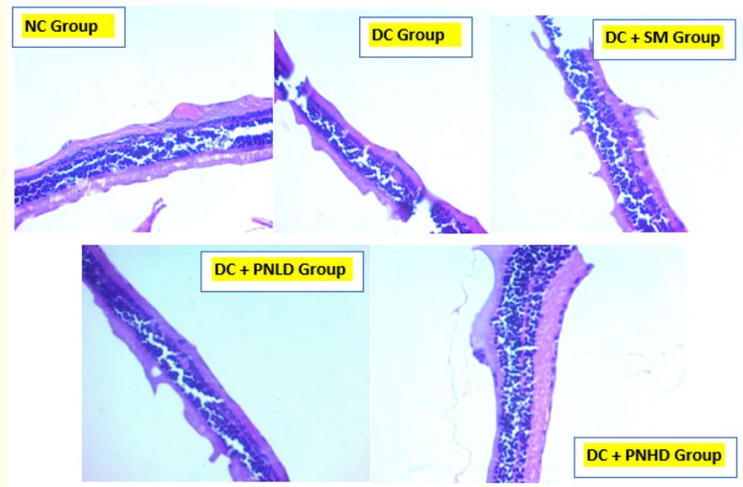


Figure 14: Histological examination and pathological features of retina.

Histopathological section of retina from normal control group showing almost normal architecture histopathological section of retina from diabetic group showing decreased number of cells in the granular layer and sloughing of other retinal layers histopathological section of retina from diabetic + Std control metformin group showing mild decrease in the number of cells in the granular layer and decrease in the size of different retinal layers histopathological section of retina from punarnavine (PN-Low) group showing decreased number of cells in the granular layer compared to diabetic group histopathological section of retina from punarnavine (PN-High) group showing mild decrease in the number of cells in the granular layer compared to diabetic group.

Histological examination and pathological features of pancreases

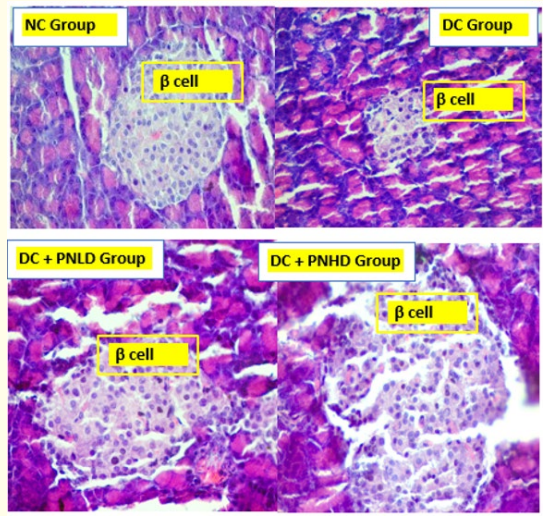


Figure 15: Histological examination and pathological features of pancreases.

Microscopic section of a pancreas from the normal Control group showing normal architecture; Microscopic section of the pancreas from the Diabetic group showing severe decrease in the population, degeneration, and necrosis of β cells compared to the control group; Microscopic section of the pancreas from the PNLD (Punarnavine Low Dose) group showing mild decrease in the population and necrosis of β cells compared to the Diabetic group; Microscopic section of the pancreas from the PNHD (Punarnavine High Dose) group showing mild decrease in the population of β cells compared to the Diabetic group.

Histological examination and pathological features of retinal vascular permeability

Retinal vascular permeability normal control group

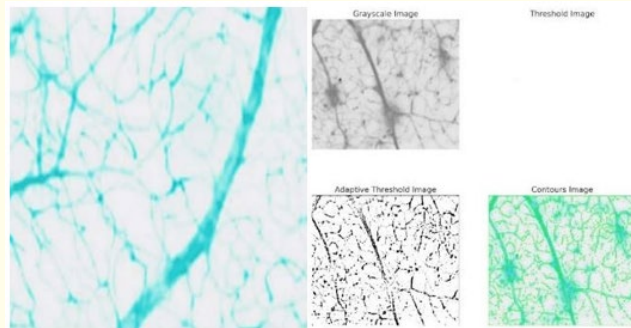


Figure 16: Normal control retinal vascular permeability grayscale image, threshold image: applied simple binary thresholding to the grayscale image; adaptive threshold image applied adaptive thresholding to handle varying lighting conditions; contours image.

Normal control grayscale image, threshold image: Applied simple binary thresholding to the grayscale image; Adaptive threshold image applied adaptive thresholding to handle varying lighting conditions; Contours image detected and drew contours on the original image. Based on the current thresholding and quantification, there were no significant stained regions detected in the normal control rat’s retinal image. The mean intensity of the detected regions (although minimal) is 2786.

Retinal vascular permeability diabetic control group

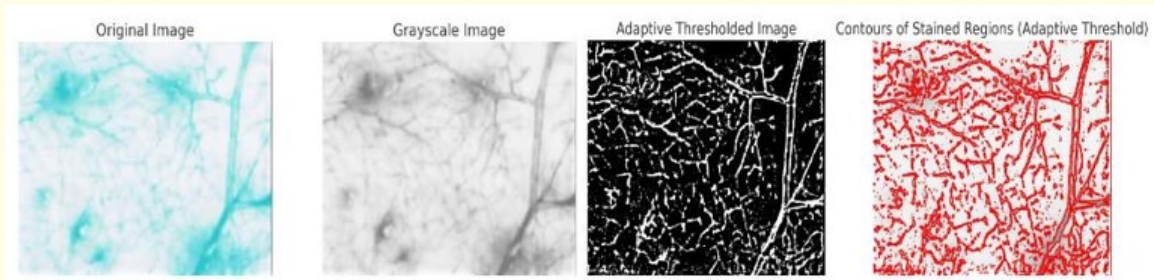


Figure 17: Diabetic control retinal vascular permeability grayscale image, threshold image: applied simple binary thresholding to the grayscale image; adaptive threshold image applied adaptive thresholding to handle varying lighting conditions; contours image.

The grayscale image of DC retinal vascular permeability using adaptive thresholding, we successfully isolated the stained regions, resulting in a total stained area of 39,483.5 square pixels. The increased retinal vascular permeability observed in the diabetic control group aligns with known pathophysiological changes in diabetic retinopathy. The total stained area of 39,483.5 square pixels suggests substantial leakage of Evans blue dye, which is consistent with the breakdown of the blood-retinal barrier often seen in diabetes. These findings support the hypothesis that diabetic conditions exacerbate vascular permeability, contributing to retinal damage.

Retinal vascular permeability PNLD

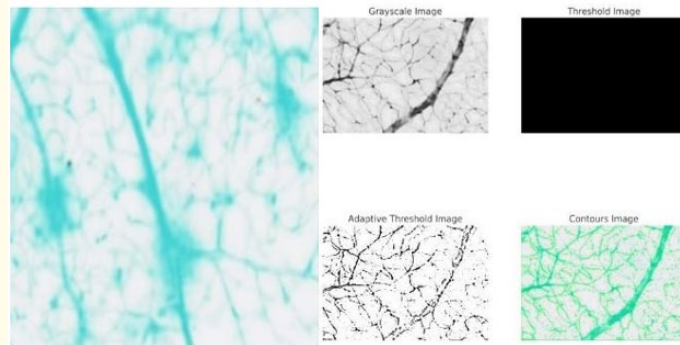


Figure 18: DC + PNLD retinal vascular permeability grayscale image, threshold image: applied simple binary thresholding to the grayscale image; adaptive threshold image applied adaptive thresholding to handle varying lighting conditions; contours image.

Punarnavine low dose treatment group grayscale image, threshold image: Applied simple binary thresholding to the grayscale image; adaptive threshold image applied adaptive thresholding to handle varying lighting conditions; contours image detected and drew contours on the original image. Based on the current thresholding and quantification, there were no significant stained regions detected in the low-dose Punarnavine-treated retinal image. The mean intensity of the detected regions (although minimal) is 2958.

Retinal vascular permeability PNHD

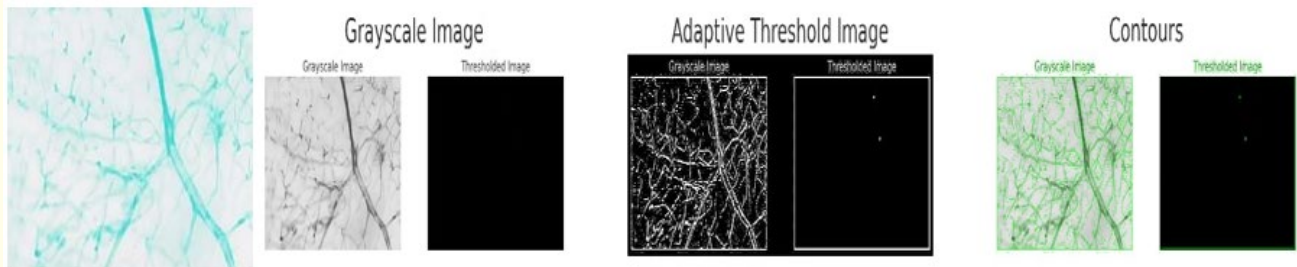


Figure 19: DC + PNHD retinal vascular permeability grayscale image, threshold image: applied simple binary thresholding to the grayscale image; adaptive threshold image applied adaptive thresholding to handle varying lighting conditions; contours image.

Grayscale image, threshold image: Applied simple binary thresholding to the grayscale image; Adaptive threshold image applied adaptive thresholding to handle varying lighting conditions; Contours image detected and drew contours on the original image. Based on the current thresholding and quantification, there were no significant stained regions detected in the high-dose Punarnavine-treated retinal image. The mean intensity of the detected regions (although minimal) is 126.5, which lies around the middle of the grayscale intensity range.

Conclusion

The findings from this study underscore the potential therapeutic benefits of punarnavine in managing diabetic retinopathy (DR) in streptozotocin (STZ)-induced diabetic rats. Punarnavine demonstrated significant antioxidant properties by reducing malondialdehyde (MDA) levels, indicating decreased lipid peroxidation, and by enhancing antioxidant enzyme activities such as catalase, superoxide dismutase (SOD), and glutathione (GSH). Specifically, high-dose punarnavine (DR+PNHD) showed robust improvements in these markers, suggesting effective mitigation of oxidative stress and reinforcement of antioxidant defences in the retina. Moreover, the assessment of vascular permeability, a crucial indicator of retinal dysfunction in DR, revealed moderate improvements in the DR+PNHD group compared to untreated DR rats. These outcomes suggest that punarnavine may contribute to stabilizing retinal vascular function and potentially mitigating the progression of diabetic retinopathy. While these results are promising, further research is needed to optimize the therapeutic regimen and to assess long-term efficacy and safety in clinical settings. Nonetheless, punarnavine emerges as a promising candidate for future therapeutic strategies aimed at managing oxidative stress and vascular dysfunction associated with diabetic retinopathy.

Disclosures

No conflicts of interest, financial or otherwise, are declared by the authors.

Author Contributions

BP, MP, KS, ZD, PL, KP, IB, DS and PP had done review of literature and experimental work. MP, PL, SK drafted manuscript; MP, BP, KS, SK, ZD, PP, DS, KP, IB evaluated and analyse the data. MP, BP, SK edited and revised manuscript; MP approved final version of manuscript.

Acknowledgement

The authors are thankful to Management of Krishna School of Pharmacy and Research, Dr. Kiran and Pallavi Patel Global University (KPGU), Vadodara, Gujarat, India for providing all the supports to carry out the research work. We also acknowledge the student start up innovation policy 2.0 (SSIP), Gujarat for providing the research grant.

Bibliography

1. Shukla UV and Tripathy K. Continuing education activity (2023).
2. Eisma JH., *et al.* "Current knowledge on diabetic retinopathy from human donor tissues". *World Journal of Diabetes* 6.2 (2015): 312-320.
3. Mishra S., *et al.* "Phytochemical, therapeutic, and ethnopharmacological overview for a traditionally important herb: *Boerhavia diffusa* Linn". *BioMed Research International* (2014): 808302.
4. Nayak P and Thirunavoukkarasu M. "A review of the plant *Boerhavia diffusa*: Its chemistry, pharmacology and therapeutical potential". *Journal of Phytopharmacology* 5.2 (2016): 83-92.
5. Krishna Murthi., *et al.* "Pharmacological properties of *Boerhavia diffusa*-a review, in editor". *International Journal of Pharmaceutical Sciences Review and Research* 5.2 (2010): 107-110.

6. Vikash A and Pankaj N. "A review of the Punarnava (*Boerhavia diffusa* Linn.): A plant with many medicinal uses".
7. Das S., et al. "Vivid phytochemical and pharmacological evaluations of *Boerhavia diffusa* L.: An omnipotent natural healer". *Systematic Reviews in Pharmacy* 14.8 (2023).
8. Sayeed S., et al. "Antidiabetic activity of roots of *Boerhavia diffusa* against streptozotocin induced diabetic rats". *Frontier Journal of Pharmaceutical Sciences and Research* 6.3 (2023): 18-24.
9. Umar R., et al. "Pharmacological properties of *Boerhavia diffusa*: A review". *International Journal of Chemical Studies* SP4 (2018): 72-80.
10. Pega-Pinto - *Boerhavia diffusa* L. [NaturezaBela.com.br]. (n.d.).
11. Shrivastava N and Padhya MA. "Punarnavine" profile in the regenerated roots of *Boerhavia diffusa* L. from leaf segments". *Current Science* 68.6 (1995): 653-656.
12. Jenkins AJ., et al. "Biomarkers in diabetic retinopathy". *The Review of Diabetic Studies: RDS* 12.1-2 (2015): 159-195.
13. Working GBD. "Biomarkers and surrogate endpoints: Preferred definitions and conceptual framework". *Clinical Pharmacology and Therapeutics* 69.3 (2001): 89-95.
14. Antonetti DA., et al. "Current understanding of the molecular and cellular pathology of diabetic retinopathy". *Nature Reviews Endocrinology* 17.4 (2021): 195-206.
15. Fung THM., et al. "Diabetic retinopathy for the non-ophthalmologist". *Clinical Medicine* 22.2 (2022): 112.
16. Panel AR. "Preferred practice pattern, diabetic retinopathy". San Francisco: American Academy of Ophthalmology (2003).
17. Emptage NP., et al. "Preferred practice pattern: Diabetic retinopathy". *American Journal of Ophthalmology* (2014).
18. Flaxel CJ., et al. "Diabetic retinopathy preferred practice pattern®". *Ophthalmology* 127.1 (2020): P66-P145.
19. Ohkawa H., et al. "Assay for lipid peroxides in animal tissues by thiobarbituric acid reaction". *Analytical Biochemistry* 95.2 (1979): 351-358.
20. Kaur I and Geetha T. "Screening methods for antioxidants-a review". *Mini Reviews in Medicinal Chemistry* 6.3 (2006): 305-312.
21. Aebi H. "Catalase". In *Methods of Enzymatic Analysis*. Elsevier (1974): 673-684.
22. Sinha AK. "Colorimetric assay of catalase". *Analytical Biochemistry* 47.2 (1972): 389-394.
23. Beauchamp C and Fridovich I. "Superoxide dismutase: improved assays and an assay applicable to acrylamide gels". *Analytical Biochemistry* 44.1 (1971): 276-287.
24. Misra HP and Fridovich I. "The role of superoxide anion in the autoxidation of epinephrine and a simple assay for superoxide dismutase". *Journal of Biological Chemistry* 247.10 (1972): 3170-3175.
25. Anderson ME. "Determination of glutathione and glutathione disulfide in biological samples". *Methods in Enzymology* 113 (1985): 548-555.
26. Rahman I and Kode A. "Oxidative stress and gene transcription in asthma and chronic obstructive pulmonary disease: antioxidant therapeutic targets". *Current Drug Targets - Inflammation and Allergy* 5.4 (2006): 375-381.

27. Skondra D., *et al.* "Characterization of azurocidin as a permeability factor in the retina: involvement in VEGF-induced and early diabetic blood-retinal barrier breakdown". *Investigative Ophthalmology and Visual Science* 49.2 (2008): 726-731.
28. Antonetti DA., *et al.* "Vascular permeability in experimental diabetes is associated with reduced endothelial occludin content: vascular endothelial growth factor decreases occludin in retinal endothelial cells. Penn State Retina Research Group". *Diabetes* 47.12 (1998): 1953-1959.
29. Diabetic Retinopathy in the Spontaneously Diabetic Torii Rat: Pathogenetic Mechanisms and Preventive Efficacy of Inhibiting the Urokinase-Type Plasminogen Activator Receptor System - Scientific Figure on ResearchGate (2024).
30. Zhang SX and Ma JX. "Ocular neovascularization: implications for age-related macular degeneration". *Molecular Vision* 13 (2007): 196-205.
31. Ma JX., *et al.* "Advanced glycation end product (AGE) accumulation on Bruch's membrane: links to age-related RPE dysfunction". *Investigative Ophthalmology and Visual Science* 46.10 (2005): 3673-3680.
32. Mihir Y Parmar., *et al.* "Neuroprotective effects of *Gymnema sylvestre* on streptozotocin- induced diabetic neuropathy in rats". *Experimental and Therapeutic Medicine* 9.5 (2015): 1670-1678.
33. Mihir Y Parmar. "Diabetes and depression: An unspeakable tale: double attack on human health". *Journal of Depression and Diabetes* 2.1 (2019): 1-3.
34. Mihir Y Parmar. "Obesity and type 2 diabetes mellitus". *Integrative Obesity and Diabetes* 4.4 (2018): 1000217.
35. Mihir Y Parmar., *et al.* "Lutein attenuates diabetic-induced renal damage via inhibiting oxidative and nitrosative stresses". *Progress in Nutrition* 19.1 (2017).
36. Mihir Y Parmar., *et al.* "Lutein dietary supplementation attenuates streptozotocin-induced testicular damage and oxidative stress in diabetic rats". *BMC Complementary and Alternative Medicine* 15 (2015): 204.
37. Ola MS., *et al.* "Neurodegeneration and neuroprotection in diabetic retinopathy". *International Journal of Molecular Sciences* 14.2 (2013): 2559-2572.
38. Aldosari DI., *et al.* "Implications of diabetes-induced altered metabolites on retinal neurodegeneration". *Frontiers in Neuroscience* 16 (2022): 938029.

Volume 13 Issue 1 January 2025

© All rights reserved by Mihir Y Parmar., et al.